Near-Infrared Colors of the Binary Kuiper Belt Object 1998 WW31 *

Naruhisa Takato (takato@naoj.org), Tetsuharu Fuse, Wolfgang Gaessler[¶], Miwa Goto[‖], Tomio Kanzawa, Naoto Kobayashi, Yosuke Minowa, Shin Oya, Tae-Soo Pyo, D. Saint-Jacque[**], Hideki Takami, Hiroshi Terada
Subaru Telescope, National Astronomical Observatory of Japan, 650 North A'ohoku Pl., Hilo, HI 96720, USA.

Yutaka Hayano, Masanori Iye, Yukiko Kamata
National Astronomical Observatory of Japan, 2-21-1 Osawa, Mitaka, Tokyo 181-8588, Japan.

A. T. Tokunaga
Institute for Astronomy, University of Hawaii, 2680 Woodlawn Dr., Honolulu, HI 96822, USA.

May 19, 2003

Abstract. We have measured near-infrared colors of the binary Kuiper Belt object (KBO) 1998 WW31 using the Subaru Telescope with adaptive optics. The satellite was detected near its perigee and apogee (0.18″ and 1.2″ apart from the primary). The primary and the satellite have similar H–K colors, while the satellite is redder than the primary in J–H. Combined with the R band magnitude previously published by Veillet et al. 2002, the color of the primary is consistent with that of optically red KBOs. The satellite's R-, J-, H-colors suggest the presence of ~ 1 μm absorption band due to rock-forming minerals. If the surface of the satellite is mainly composed by olivine, the satellite's albedo is higher value than canonically assumed value of 4%.

Keywords: Kuiper Belt Objects, binary, near-infrared color, adaptive optics system

1. Introduction

Kuiper belt objects (KBOs) are thought to be remnants of solar system formation (Edgeworth 1949; Kuiper 1951). These bodies might have physical or chemical information about the early stage of the solar sys-

[¶] Current address: Max-Plank-Institute für Astronomie, Königstuhl 17, Heidelberg D-69117, Germany.

[‖] Visiting astronomer at Institute for Astronomy, University of Hawaii, 640 North A'ohoku Pl., Hilo, HI 96720, USA.

[**] Current address: Groupe d'astrophysique, Université de Montréal, 2900 Boul. Édouard-Monpetit, Montréal (Québec) H3C 3J7, Canada.

[*] Based on data collected at Subaru Telescope, which is operated by the National Astronomical Observatory of Japan.

tem. Recently, several KBOs were identified as binary systems (Veillet et al. 2002 and references therein). The binary KBOs are important because we can derive the total mass of the systems and constrain its density by assuming the albedo.

1998 WW31 was the first KBO identified as a binary system other than the Pluto-Charon system (Veillet et al. 2002). The orbit of the satellite is highly eccentric (e=0.82) and has a long period (P=574 days), which is not similar to that of the Pluto-Charon system (e=0.0, P=6.4 days). However, the obliquities are both large (1998 WW31 system: 65.°2, Pluto-Charon system: 119.°6 (Tholen & Buie 1997). The total mass derived from its orbit is 2.7×10^{18} kg (1/5000 of Pluto-Charon system). The diameter of the primary and the satellite is estimated to be 118–148 km and 98–123 km, respectively, assuming that they have the same density 1.0–2.0 g cm^{-3} and albedo.

The origin of the binary KBOs is not known. A giant impact scenario has been proposed for Pluto-Charon system (McKinnon 1989; Stern et al. 1997). If this is the case for the 1998 WW31 system, the impact may have fragmented the original KBO such that its interior is now exposed. However, the collisions were too infrequent to account for the observed number of binaries (Weidenschilling 2002; Stern 2002; Goldreich et al. 2002). Stern (2002) pointed out that if the albedos of the primary and/or the satellite are higher than the canonical assumption of 4%, the estimated size of the primary and/or the satellite are reduced and the frequency of the collision is enough to produce the observed number of KBO binaries. In this paper, we report the near-infrared photometry of the primary and the satellite of 1998 WW31 system, and discuss the difference of the surface compositions.

2. Observations and Reductions

The J- (1.17–1.33 μm), H- (1.48–1.78 μm), and K- (2.03–2.37 μm) band (Tokunaga et al. 2002) photometry was obtained during the commissioning run of the adaptive optics (AO) systems (Takami et al. 1998) on Oct. 31, 2001(UT) at the f/12.4 Cassegrain focus of the Subaru Telescope on Mauna Kea, using the Infrared Camera and Spectrograph (IRCS: Kobayashi et al. 2000, Tokunaga et al. 1998). The AO system is a curvature sensing system with 36 actuators. IRCS uses an 1024×1024 pixel InSb array with a pixel scale of $0.058''$ pixel^{-1}.

The night was photometric. The natural seeing was about $0.5''$ FWHM at K-band. Since 1998 WW31 was too faint for the wavefront reference for the AO system, we used V=11.5 mag star GSC0124300262 as the

Table I. Journal of observation.

Time UT 2001 Oct. 31	Filter	Air mass	Exp(sec)×frames	Separation from ref. star (″)
1998 WW31[a]				
9:00 - 9:36	J	1.22 - 1.17	300× 6	8.5 - 10.1
9:43 - 10:34	H	1.09 - 1.04	180×15	10.4 - 12.7
10:39 - 10:56	K	1.02	180× 5	12.9 - 13.7
10:59 - 11:16	H	1.01	180× 5	13.8 - 14.6
11:51 - 13:00	K	1.00 - 1.05	180×20	16.2 - 19.3
Standard star [b]				
13:24 - 13:33	K	1.06	50× 5	···
13:35 - 13:40	H	1.06	20× 5	···
13:42 - 13:48	J	1.06	20× 5	···

a: r=46.78 AU, Δ=45.84 AU, α=0.°39

b: Imaging through AO optics but without correction.

wavefront reference. The distance between the KBO and the reference star was 8.5″ at the beginning of the observations and 19″ at the end[1].

At the time of the observations the orbital elements were not published, and we expected a larger separation than we actually observed. As a result, we set the exposure time long enough for the frame to become background noise limited. It was 300 sec. for J-band and 180 sec. for H- and K-band. But the object moved 0.23″ in the J-band exposures and 0.14″ in the H- and the K-band exposures, which makes the images elongated. Fortunately, 1998 WW31 moved nearly perpendicular to the direction to the satellite, and we could resolve the primary and its satellite.

Flat fields were constructed for each filter using the median of the science images. We used a five-point dithering pattern with 3″ separation (like the pip pattern for five on dice) by using the AO system's tip/tilt mirror. Good quality images were selected for maximizing the spatial resolution and shifted based on the calculated position of the object and averaged. The total exposure times of the final images are 1800 sec., 1440 sec. and 3240 sec. for J-, H- and K-band, respectively (Figure 2). For estimating the image resolution, we also combined images of a star. The FWHM of the combined image is 0.14″, 0.20″ and 0.19″ for J-, H-, and K-band, respectively, measured with a star

[1] We used HORIZON maintained by JPL (`http://ssd.jpl.nasa.gov/`) to predict the position of 1998 WW31.

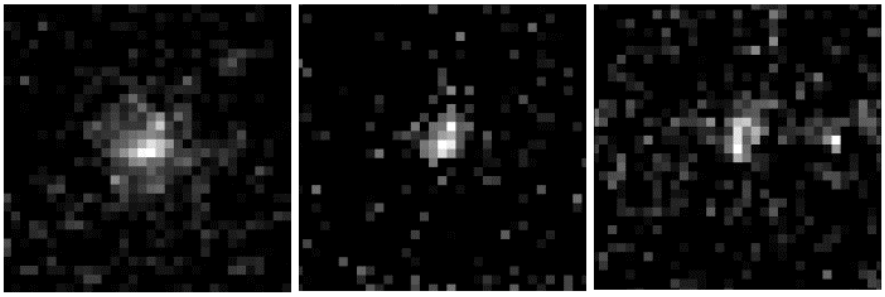

Figure 1. Near-infrared images of 1998 WW31 system (left: J, center: H, right: K). North is up and east is to the left. Field of view is $3.7''$ square for each band. Images are elongated nearly east–west direction, because of the motion of the object during each exposure frame (see text).

Table II. Relative position of the satellite of 1998 WW31 (measured on J-band image).

DATE	JD	$\Delta\alpha$ $('')^{a,b}$	$\Delta\delta$ $('')^{a,b}$	Sep. $('')$	P.A.$(^\circ)$
UT 2001 Oct. 31	2452213.89	$-0.06\pm_{0.12}$	$0.17\pm_{0.06}$	0.18	-18

a: (position difference) = (satellite position) − (primary position)

b: Assigned error is ±2 pixels and ±1 pixel for $\Delta\alpha$ and $\Delta\delta$, respectively.

which was $34''$ apart from the wavefront reference star. Photometric calibration was obtained using standard star GSPC_S840-F (Persson et al. 1998). Table I shows the journal of our observations.

Magnitudes of the primary and the satellite were calculated from the total magnitude and the magnitude difference.

Photometry was performed to measure the total magnitude of the 1998 WW31 system. We obtained the aperture size vs. flux curve to find a plateau in the aperture photometry and determined the total flux by averaging the flux at aperture size of $1.16''$, $1.28''$ and $1.39''$ in diameter for J- and H-band. There was no clear plateau in the K-band photometry, we adopted the average of the flux measured at the same apertures as for J- and H-band. The sky was calculated from annular region with $1.74''$ in inner diameter and $0.58''$ in width. We measured the errors of the photometry by taking the same aperture to measure standard deviation of the flux in the blank sky surrounding the object.

The magnitude difference between the primary and the satellite was measured based on the peak intensity ratio. Since the point-spread

function (PSF) of the primary and the satellite are identical (the separation between the two bodies was small enough within the iso-planatic angle), the peak intensity ratio is the same as the flux ratio of the two bodies. To improve the signal to noise ratio, we applied aperture photometry with small apertures ($0.12''$ to $0.23''$ in diameter) around the peak of each object. To calculate the satellite peak flux, the flux contribution from the primary at the satellite's position should be subtracted from aperture photometry data of the satellite. We assumed that the PSF of the primary was symmetric with respect to the east-west direction (the axis of the symmetry is parallel to the object motion), and we used the flux at the mirrored position of the satellite as the flux from the primary at the satellite position. The satellite's contribution to the peak flux of the primary was also subtracted as the same way. We used the maximum difference of the flux ratio measured by several small apertures to determine the error.

3. Discussion

The satellite's position and the results of the photometry are summarized in Table II and Table III. Heliocentric and geocentric distance correction were applied to the R-band magnitude from Veillet et al.(2002). The satellite was detected at $0.17''$ north and $0.06''$ west of the primary position. This is in agreement with the position predicted by Veillet et al. (2002) to within 1 pixel (58 mas) (Figure 3).

We computed the reflectivity of the primary and the satellite from the photometric data using the adopted solar colors V–R=0.36, V–J=0.108, J–H=0.29, and H–K=0.06 (Hartmann et al. 1982; Hartmann et al. 1990; Hardorp 1980). Possible magnitude variations with rotation of the primary and the satellite are not taken into consideration. Figure 3 shows the reflectivity normalized by the H band reflectivity.

The colors of these optically red KBOs are thought to be compatible with carbon-rich compounds, organics extract from the Murchison meteorite (Clark 1982; Moroz et al. 1998), or "tholins" (Khare et al. 1984; Wilson et al. 1994). The primary of 1998 WW31 has steep, red optical color, consistent with the colors of other known KBOs.

On the other hand, the satellite has large J–H and small R–J values. Although the signal-to-noise ratio is low, the J–H color suggests that the normalized reflectivity of the satellite is lower than the primary in between R- to J-band region. This color is difficult to explain by the same organic materials. Cruikshank et al. (1998) mentioned that it is hard to explain the 0.9–1.3 μm spectrum of 5145 Pholus by assorted

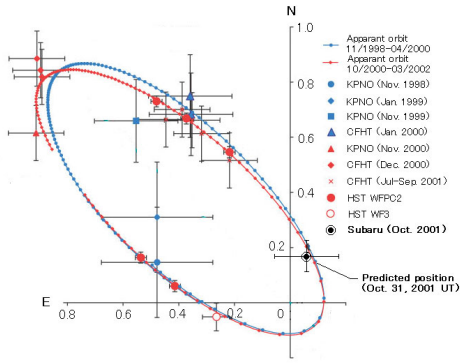

Figure 2. Relative position of the satellite. The orbit and data points except ours are reproduced from Veillet et al. (2002).

Table III. Results of photometry.

	Magnitudes and colors (mag)						
	R [a]	J	H	K	$R-J$	$J-H$	$H-K$
Total	23.5±0.1	22.19±0.13	21.55±0.17	21.83±0.28	1.31±0.16	0.64±0.21	−0.28 ±0.33
Δm	0.4±0.1	0.92±0.08	0.12±0.07	0.04±0.20	···	···	···
Primary	24.07±0.1	22.58±0.15	22.24±0.18	22.56±0.34	1.49±0.21	0.34±0.23	−0.32±0.38
Satellite	24.47±0.1	23.49±0.15	22.36±0.18	22.60±0.34	0.98±0.21	1.13±0.23	−0.24±0.38

	Reflectivity normalized by H band [b]			
Primary	0.47±0.07	0.95±0.14	1±0.18	0.70±0.26
Satellite	0.36±0.05	0.46±0.07	1±0.18	0.76±0.28

a: Veillet et al.(2002) with heliocentric and geocentric distance correction of −0.1 mag.
b: Adopted solar colors: $V-R=0.36$, $V-J=1.08$, $J-H=0.29$, and $H-K=0.06$ (Hartmann et al. 1982; Hartmann et al. 1990; Hardorp 1980).

carbon-rich materials, and suggest the presence of 20-μm grains of olivine.

The large J–H color might be explained by the broad Fe^{2+} absorption band near 1 μm of rock-forming minerals such as olivine, pyroxene, and amphibole group. Figure 4 shows the reflectance spectra of the satellite of 1998 WW31 compared with that of "space weathered" olivine grain obtained by laboratory experiments normalized at the V band reflectivity (Sasaki et al. 2001), together with the spectra of A-type asteroid 863 Benkoela and the small KBO 1995 HM5 (B, V, R, I, J, and H) (Barucci et al. 2000; Boehnhardt et al. 2001). The space weathering was simulated by applying short laser pulse on the olivine

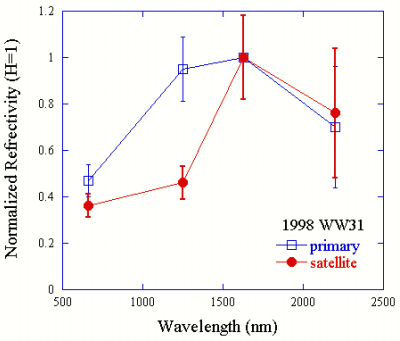

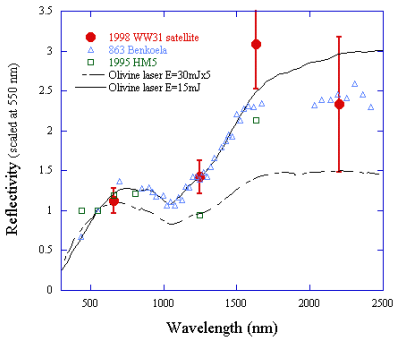

Figure 3. (*Left*) Normalized reflectivity vs. wavelength for the primary and the satellite of 1998 WW31 system. The reflectivity are normalized by the H-band values. The R-band magnitudes are taken from Veillet et al. (2002) with heliocentric and geocentric distance corrections.

Figure 4. (*Right*) Reflectivity of the satellite of 1998 WW31 compared with olivine-rich clan of S-type asteroid 863 Benkoela and "space weathered" olivine simulated in laboratory (Sasaki et al. 2001). Two thin lines represent the olivine powder reflectivity after pulse laser irradiations (30 mJ $\times$ 5 and 15 mJ). The spectra are scaled at 550 nm. The reflectivity of small KBO 1995 HM5 are also plotted (Barucci et al. 2000; Boehnhardt et al. 2001). The reflectivity of the satellite are scaled to the "olivine 30 mJ $\times$ 5" spectrum at 1250 nm. The R band reflectivity is taken from Veillet et al. (2002) with heliocentric and geocentric distance corrections.

grains. The satellite reflectivity is scaled to the reflectivity of olivine subjected to five times of a 30 mJ laser at 1.25 μm.

The J–H color of the satellite is compatible with the "space weathered" olivine. There are some other KBOs which seems to have compatible spectra with a 1 μm absorption band. 1995 HM5 is a KBO with 130 km equivalent diameter (assuming its albedo is 0.04) and has a red J–H color, though very uncertain. The optical to near-infrared color is also compatible with the spectra of space-weathered olivine. The KBO 1999 DE9 also shows consistency with olivine absorption (Jewitt and Luu 2001).

We cannot specify the composition of the satellite surface from broadband photometry. However, the 1 μm absorption feature of rock-forming minerals including olivine is one of the possible candidates that explain the R-, J-, H-band color of the satellite. Since the albedo of the olivine is high, if we adopt the olivine as the surface composition of the satellite, the surface albedo of the satellite should be significantly higher value of 20–40% (Sasaki et al. 2001) than the canonical assumption of 4%. This implies that the diameter of the satellite is 2–3 times smaller

than considered before, and the binary formation by collision can be valid (Stern 2002).

References

Barucci, M. A., Romon, J., Doressoundiram, A., & Tholen, D. J. 2000, *Astron. J.*, 120, 496

Boehnhardt, H., Tozzi, G. P., Birkle, K., Hainaut, O., Sekiguchi, T., Vair, M., Watanabe, J., Rupprecht, G., & The FORS Instrument Team 2001, *Astron. Astrophy.*, 378, 653

Clark, R. N. 1982, Icarus, 49, 244

Cruikshank, D. P., Roush, T. L., Bartholomew, M. J., Geballe, T. R., Pendleton, Y. J., White, S. M., Bell, J. F. III, Davies, J. K., Owen, T. C., de Bergh, C., Tholen, D. J., Bernstein, M. P., Brown, R. H., Tryka, K. A., & Dalle Ore, C. M. 1998, Icars, 135, 389

Edgeworth, K. E. 1949, *M. N. R. A. O.* , 109, 600

Goldreich, P., Lithwich, Y., & Sari, R. *Nature*, 420, 643

Hardorp, J. 1980, *Astron. Astrophy.*, 91, 221

Hartmann, W. K., Cruikshank. D. P., & Degewij, J. 1982, Icarus, 52, 377

Hartmann, W. K., Tholen, D. J., Meech, K. J., & Cruikshank, D. P. 1990, Icarus, 83, 1

Jewitt, D. C. & Luu, J. X. 2001, *Astron. J.*, 122, 2099

Khare, B. N., Sagan, C., Arakawa, E. T., Suits, F., Callcott, T. A., & Williams, M. W. 1984, Icarus, 60, 127

Kuiper, G. P. 1951, Astrophysics, J. A. Hynek, McGraw-Hill: New York, 357

McKinnon, W. B. 1989, *Astrophy. J.*, 344, 41

Kobayashi, N., Tokunaga, A., Terada, H., Goto, M., Weber, M., Potter, R., Onaka, P., Ching, G., Young, T., Fletcher, K., Neil, D., Robertson, L., Cook, D., Imanishi, M., & Warren, D. 2000, Proc. SPIE, 4008, 1056

Moroz, L. V., Arnold, G., Korochantsev, A. V., & Wäsch, R. 1998, Icarus, 134, 253

Persson, S. E., Murphy, D. C., Krzeminski, W., Roth, M., & Rieke, M. 1998, *Astron. J.*, 116, 2475

Sasaki, S., Nakamura, K., Hamabe, Y., Kurahashi, E., & Hiroi, T. 2001, Nature, 410, 555

Stern, S. A., McKinnon, W. B., & Lunine, J. 1997, Pluto and Charon, S. A. Stern & D. J. Tholen, The University of Arizona Press: Tucson, 605

Stern, S. A. *Astron. J.* 124, 2300

Takami, H., Takato, N., Otsubo, M., Kanzawa, T., Kamata, Y., Nakashima, K., & Iye, M. 1998, Proc. SPIE, 3353, 500

Tholen, D. J. & Buie, M. W. 1997, Pluto and Charon, S. A. Stern & D. J. Tholen, The University of Arizona Press: Tucson, 193

Tokunaga, A. T., Kobayashi, N., Bell, J., Ching, G. K., Hodapp, K., Hora, J. L., Neil, D., Onaka, P. M., Rayner, J. T., Robertson, L., Warren, D. W., Weber, M., & Young, T. T. 1998, Proc. SPIE, 3354, 512

Tokunaga, A. T., Simons, D. A., & Vacca, W. D. 2002, *P. A. S. P.*, 114, 180

Veillet, C., Parker, J. W., Griffin, I., Marsden, B., Doressoundiram, A., Buie, M., Tholen, D. J., Connelley, M., & Holman, M. J. 2002, Nature, 416, 711

Icars 160, 212

Wilson, P. D., Sagan, C., & Thompson, W. R. 1994, Icarus, 107, 288